Analysis of Electromagnetic Forces in High Voltage Superconducting Fault Current Limiters with Saturated Core

Jaime Cabanes Aracil[1], Jose Lopez-Roldan[2], Jacob Carl Coetzee[3], Frank Darmann[4] and Tee Tang[5]

[1,3,5] School of Electrical Engineering and Computer Science, Queensland University of Technology, Gardens Point Campus, P.O. Box 2434, 2 George Street, Brisbane Q4001 Australia

[2,4] ZenergyPower Pty Ltd. Suite7, 1 Lowden Square Wollongong NSW 2500 Australia

Email: jaime.cabanes@qut.edu.au (Corresponding author)

Abstract- This paper presents a three-dimensional numerical analysis of the electromagnetic forces within a high voltage superconducting Fault Current Limiter (FCL) with a saturated core under short-circuit conditions. The effects of electrodynamic forces in power transformer coils under short-circuit conditions have been reported widely. However, the coil arrangement in an FCL with saturated core differs significantly from existing reactive devices. The boundary element method is employed to perform an electromagnetic force analysis on an FCL. The analysis focuses on axial and radial forces of the AC coil. The results are compared to those of a power transformer and important design considerations are highlighted.

Keywords- Fault Current Limiter; boundary element method; short-circuit; electromagnetic forces

I. INTRODUCTION

FAULT Current Limiters act as high-voltage surge protectors for power grids, increasing system reliability and efficiency and enabling cost-efficient grid expansion, including the integration of distributed generation sources [1], [2]. High Temperature Superconductor (HTS) fault current limiting concepts have recently been receiving a lot of attention [2-6]. The successful implementation of an HTS saturated core FCL was reported in [7]. Figure 1 shows the basic arrangement of the saturated core HTS FCL. It consists of two iron cores with conventional copper AC coils wound on the cores and a superconductor DC coil wound around them. The circuit that needs to be protected is connected in series with the AC coils of the FCL. An HTS DC coil enclosing both cores is used to bias the cores into saturation under normal operating conditions, thereby providing a low steady-state inductance. Under a fault condition, the biasing by the HTS DC coil is reduced in response to the increased current in the load, thus causing the cores to become unsaturated. The inductance of the HTS FCL changes

instantly to a high value, thereby limiting the fault current to a prescribed maximum. A two coil-core structure per phase is needed to limit the AC current. When the AC fault current is positive, the first coil-core structure limits the current. On the other hand, the fault current is restricted by a second coil-core structure wound in the opposite direction when the AC current is negative. Table 1 and Figure 2 show the fault current with and without an FCL under short-circuit conditions used by ZenergyPower Ltd Pty [8]. The peak of the fault current is reduced significantly.

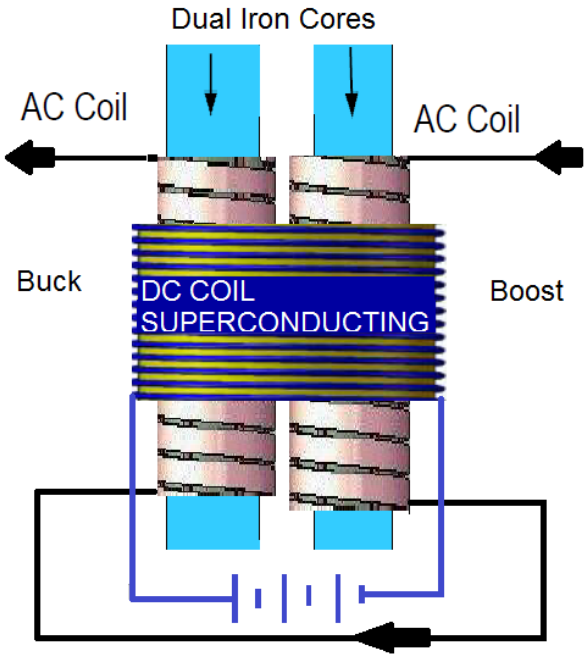

Figure 1 The basic saturating reactor HTS fault current limiting concept diagram

Parameter	Value
Rated voltage	11.3 kV
Line frequency	50 Hz
Prospective unlimited peak fault current	17 kA peak
Peak limited current (with FCL)	13.25 kA peak
Prospective unlimited symmetrical fault current	6.2 kA rms
Limited symmetrical current (with FCL)	5 kA rms

Table 1 Circuit design parameters

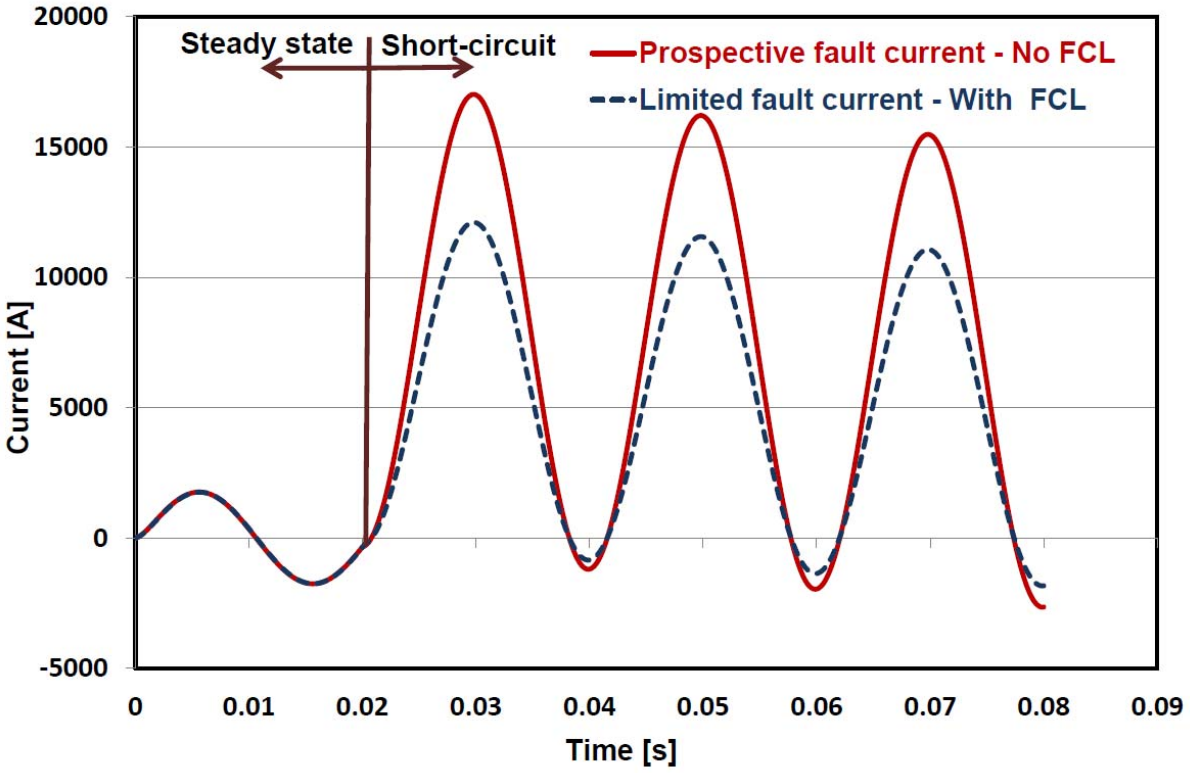

Figure 2 Prospective and limited fault current.

Electromagnetic forces can be very severe in high voltage applications. A power-transformer under short circuit condition has to withstand significant internal forces, caused by the high currents in the transformer windings. These electromagnetic forces present as radial and axial forces [9-11]. Analysis of electromagnetic forces within a power-transformer is well established [9-19]. It was shown that such forces are potential sources for damage. The windings are subjected to hooping stress, buckling, tilting, axial or radial bending. Techniques to mitigate the electrodynamic stresses in power transformers have been proposed in [9, 11]. The fundamentals of these techniques (spacers, wrapping, CTC dimension) can be extrapolated to the coils in an FCL, since the construction and manufacturing of the coil is very similar.

For different applications, the design of an FCL has to be considered individually to ensure that the structure is able to withstand the effects of the high forces. The problem faced when applying the models used in the analysis of power transformer on FCL design is that transformer models are generally based on round core-coil arrangement [9-19], whereas FCL cores and coils often have different geometries. Since fault current limiting for high voltage applications is a relatively new technology, the effects of electromagnetic forces in HTS FCL coils have never been reported. The purpose of this paper is to analyse these forces and to compare results with

those in round coils of power transformers under short-circuit conditions. Commercial software based on the Boundary Element Method (BEM) is used for this purpose.

II. ELECTROMAGNETIC FORCES IN TRANSFORMER WINDINGS

The distribution of electromagnetic forces (Lorentz Forces) is a function of the current density in the conducting regions and magnetic flux density in the same region. Mathematically, this can be represented as [11]

$$\mathbf{F} = \mathbf{J} \times \mathbf{B} \tag{1}$$

where **F** is the force density vector**.** Due to the cross product relation, the direction of the force will be perpendicular to both the current density and the flux density vectors.

In order to get a better understanding of the electromagnetic forces in an FCL, it is necessary to consider these forces within a power transformer. Under a short-circuit conditions, the electromagnetic forces exerted in the windings of a power transformer reach a maximum and may cause severe damage to the structure. The main forces are axial (compression) and radial (hooping and buckling) [9]. Several authors have developed formulations to compute the average and maximum values of these forces in round-core power transformers. Both the analytical formulations [9],[10],[12] and the 3D numerical analysis Finite-Element-Method analysis [15, 20, 21] obtained similar force patterns within the windings of a power transformer.

In this paper, the boundary element method (BEM) is used to conduct the force analysis. In BEM, the differential equation formulation for the electric potential is not solved directly. An equivalent source is sought which will sustain the field as prescribed by an appropriate set of boundary conditions applied to a specific function (called the Green function) which relates the location and effect of the source to any point on the geometry. This approach has the advantage over the finite element method in that it is not constrained by conventional domain dividing grids. This allows greater accuracy with geometrical representation. Once the source has been determined, the potential or derivatives of the potential can be calculated at any point. The commercial software calculates the magnetic vector potential **A** due to an arbitrarily oriented surface current density **J** from [21-23]

$$\mathbf{A}(\mathbf{r}) = \mu_o \int_s \boldsymbol{G}(\mathbf{r}, \mathbf{r}')\mathbf{J}(\mathbf{r}')d\mathbf{s}' \,, \tag{2}$$

where *G* is the Green function, given by

$$\boldsymbol{G}(\mathbf{r}, \mathbf{r}') = \frac{1}{4\pi|\mathbf{r}-\mathbf{r}'|} \,. \tag{3}$$

In the case of a magnetostatic field, the magnetic flux density is determined from

$$\mathbf{B} = \nabla \times \mathbf{A} . \tag{4}$$

For comparison, a 3D model of a simple concentric winding power transformer was created and analysed. In order to make a comparison between the power transformer and the HTS FCL, the following assumptions were made:

- Both systems have the same sizes in terms of core height, coil height, coil radial dimensions and main clearances (see Table 2).
- Both systems are configured for a 3-phase circuit and are modelled in three dimensions.
- Both systems have nonlinear cores with a saturation flux density of B_{sat}=1.82 T at H_{sat} =800 A/m.
- Both systems are simulated without an oil tank.

Parameter	**PT Value**	**FCL Value**
AC magnetomotive force (mmf)		500 kAT
DC magnetomotive force (mmf)		250kAT
AC magnetomotive force (mmf) High Voltage (HV)	500kAT	
AC magnetomotive force (mmf) Low Voltage (LV)	250kAT	
Nominal current value	1170Arms	1170Arms
Core height	2.1m	
AC coil height	2m	
Core Area	0.84m2	

Table 2 Model design parameters

Figure 3 shows a partial image of the magnetic leakage field of simple concentric windings in a power transformer. The resultant force will depend on the flux direction. Hence the force will be vertically oriented (axial) at the top and bottom of the coil and horizontal (radial) at the centre.

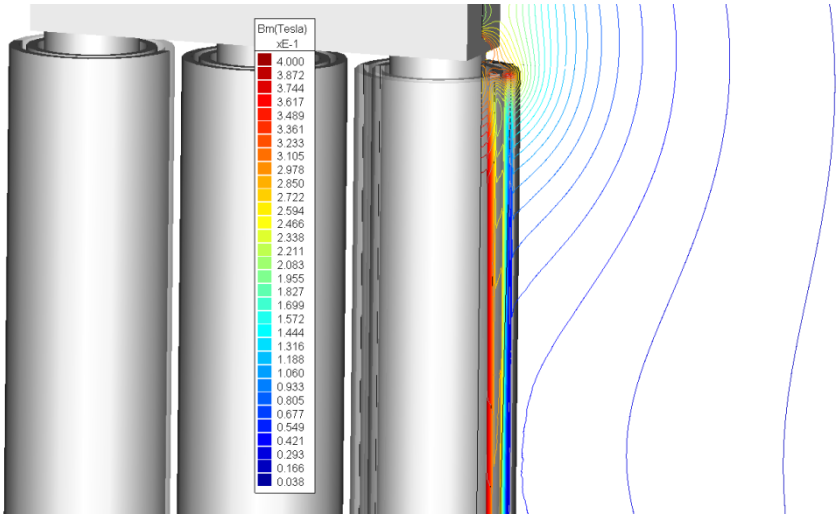

Figure 3 Magnetic leakage flux within a standard three-phase power transformer.

Figure 4 shows the axial and radial force behaviour within the winding of a typical power transformer during a fault. The *x*-axis refers to the normalised longitudinal position along the coil, that is, 0 is the bottom of the coil and 1 is the top of the coil.

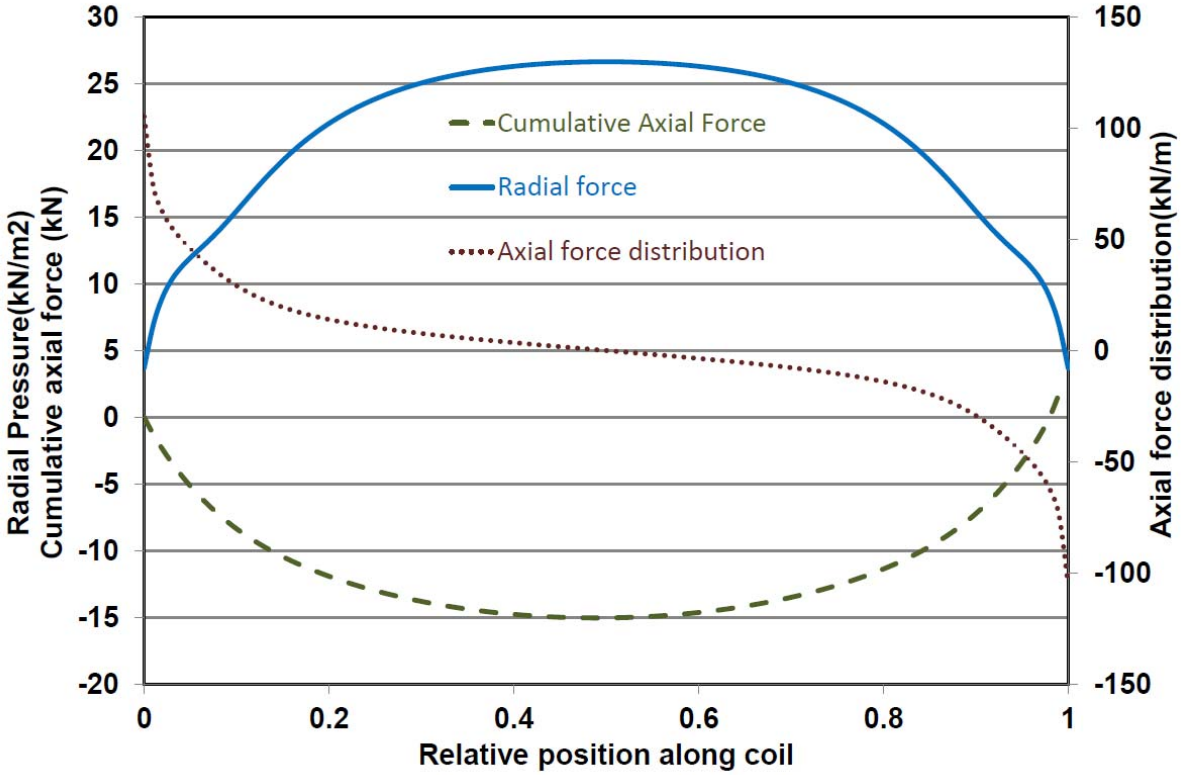

Figure 4 Electromagnetic forces within a standard three-phase power transformer under short-circuit conditions.

In a power transformer, the radial forces are low at the ends of the winding and very high at the centre of the winding, as shown in Figure 4. This force is expressed in terms of radial pressure in Figure 4. The maximum pressure observed is 27 kN/m^2 at the centre of the coil. On the other hand, the axial force is very high at the ends of the winding and zero in the turns located at the centre. Figure 4 also shows the axial cumulative force, which is the integral of the axial force distribution. The axial cumulative force therefore increases rapidly at the ends of the windings and is stable at the centre, resulting in a maximum compression of the coil of 15 kN.

III. ELECTROMAGNETIC FORCES IN FAULT CURRENT LIMITERS

The aim is to determine the peak force in the AC coils that a High Voltage FCL has to withstand when a short-circuit fault occurs. In order to perform this static analysis, a short-circuit condition is simulated. The greatest force is expected at the peak of the asymmetric fault current. Hence a current peak of 13.25 kA is applied to the AC coils. Radial forces and axial forces are studied in the different parts of the AC coils. The AC coils are

wound in opposite directions. The fields of the coils will interfere, thus affecting the resultant force. It is therefore important to differentiate between the different parts of the coil arrangement.

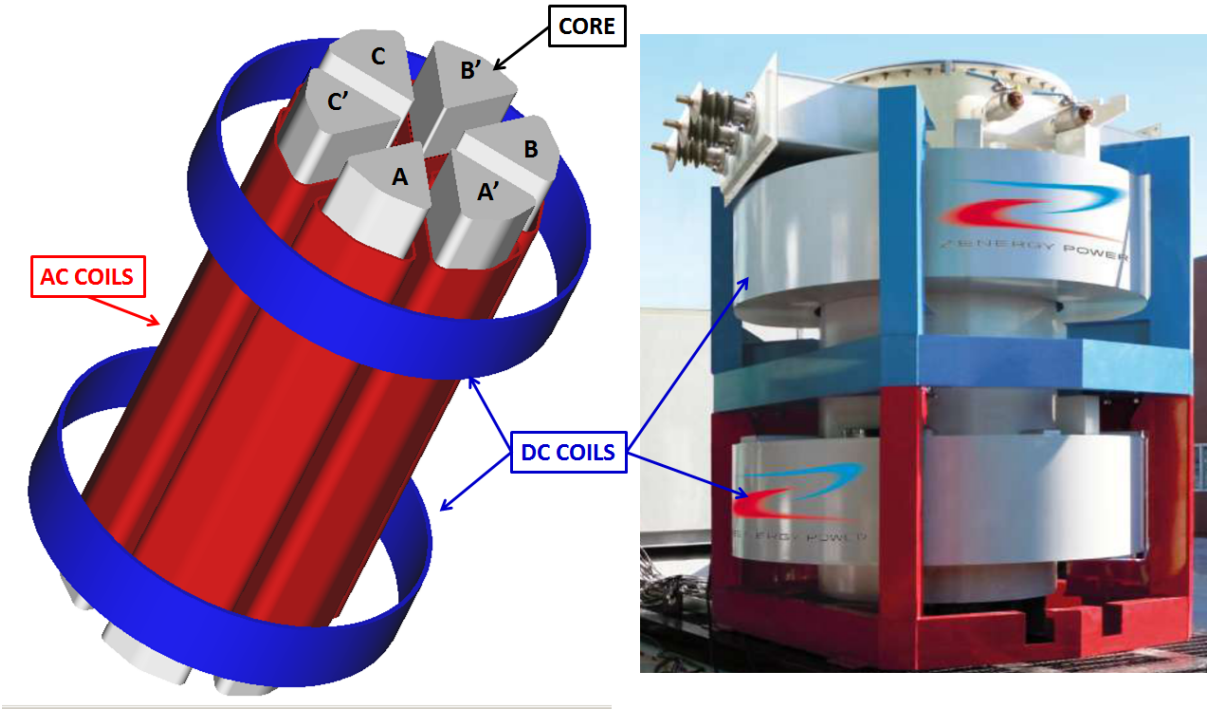

Figure 5 General geometry of the HTS FCL.

The geometry of the HTS FCL is shown in Figure 5. The example considered is an open core FCL designed by ZenergyPower Ltd Pty. This design has DC superconductors around the AC coils, as explained in Figure 1. The superconducting DC coil is divided in two parts. This FCL model is designed to reduce a three phase fault. It therefore has six cores, since two cores-AC-coils per phase are required (Phase A-A', B-B' and C-C'). Each core is therefore independent and unconnected through a yoke, as shown in Figure 5. The total magnetic field within the FCL is driven by the three phases. The influence of every phase thus needs to be taken into account in the calculation of the total magnetic flux.

The saturated core FCL with HTS DC bias coil was analysed using 3D BEM. Figure 6 shows a partial image of magnetic leakage field pattern in the FCL. The current in the DC coils give rise to magnetic flux around them.

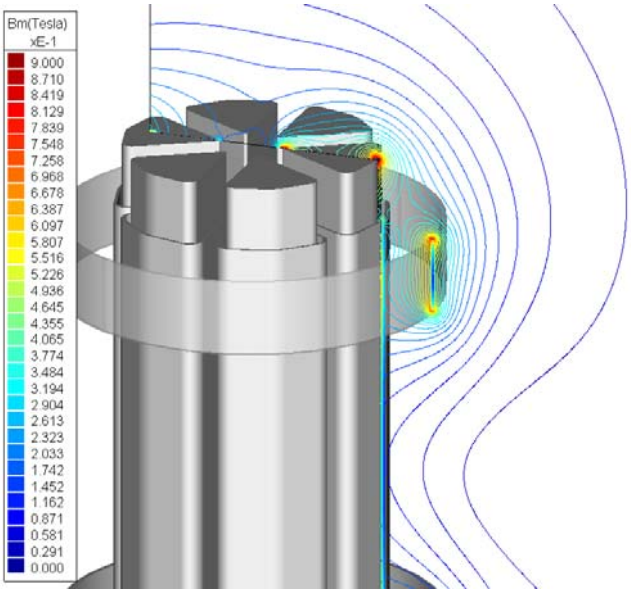

Figure 6 Magnetic leakage flux within the FCL.

The magnetic flux created by the DC coils boosts the magnetic flux in the AC coil where it faces a DC coil. This results in an increase in the radial force, as shown in Figure 7(a).

Figure 7 represents the radial volumetric forces on the surface of the AC coil. Figure 7(a) represents the FCL with the DC coils activated while Figure 7(b) shows the force with the DC coils disabled. The maximum volumetric force (red area) is located in the area facing the DC coils. Positive values of force represent an expansion force, while negative values indicate compression forces.

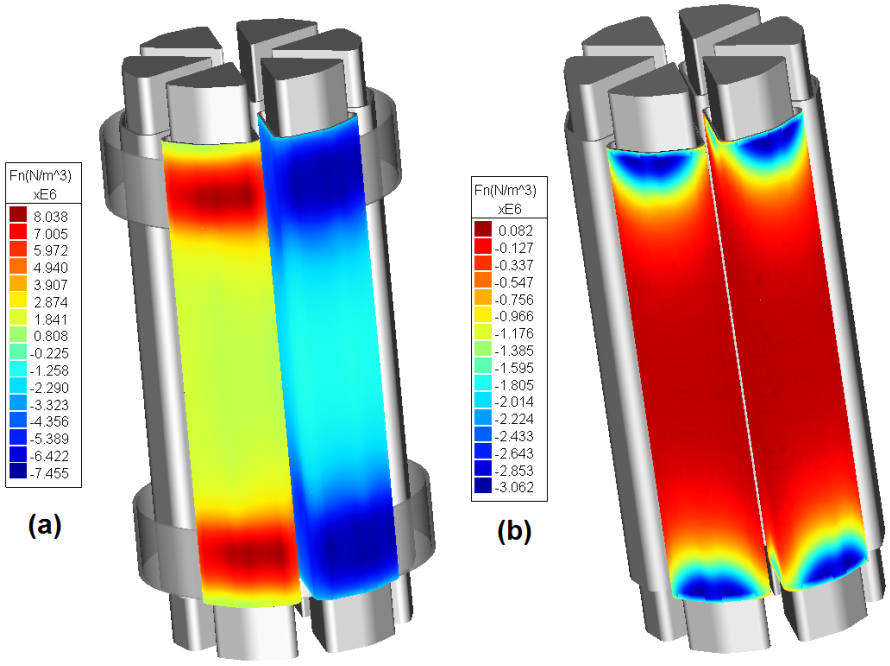

Figure 7 Magnetostatic image of the volumetric radial force in the AC coils of the HTS FCL

Figure 8 shows the radial force distribution plotted against position along the AC coil. The maximum peak occurs in the AC coil area facing the DC coil when the AC current is flowing in the same direction as the DC current (positive AC current). In this case, the magnetic fields due to the DC and AC coils are in the same direction, and therefore interfere constructively. The analysis was conducted for the two windings belonging to Phase 1.

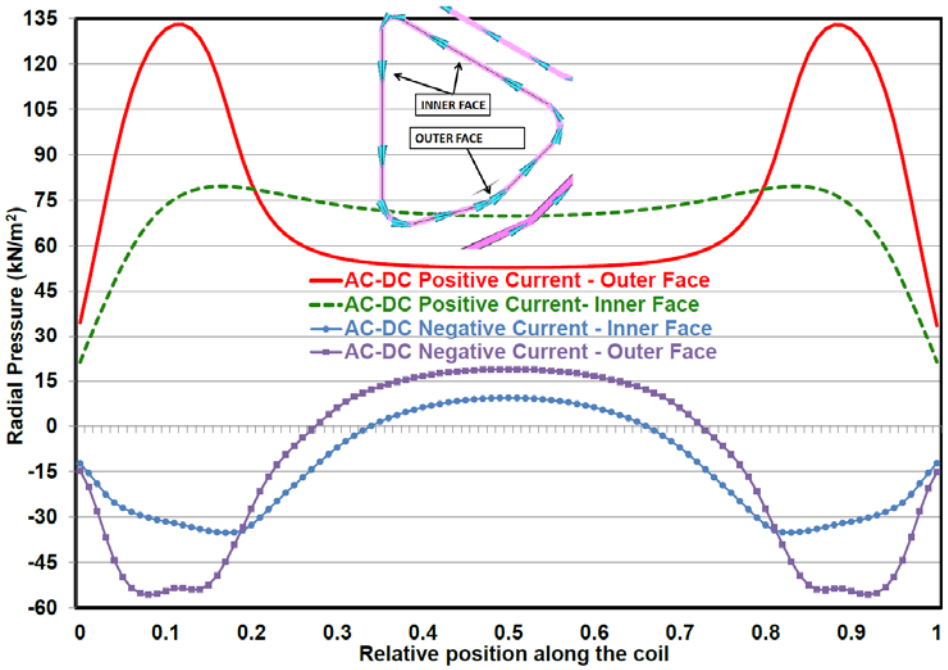

Figure 8 Radial force distribution along the AC coil.

A positive pressure implies expansion, which cause a hooping effect in the winding. On the other hand, negative pressure implies compression, which causes buckling stresses in the winding.

The axial force analysis was also conducted to determine the compression forces in the coils and the clamping. Figure 9 shows the axial volumetric force distribution on the surface of the AC coil. The maximum volumetric force occurs on the edges at the bottom and the top of the AC coils.

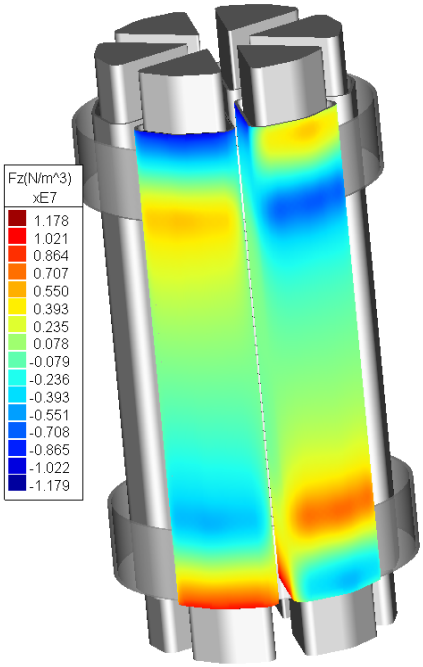

Figure 9 Volumetric axial force in the AC Coils of the HTS FCL

For the axial force analysis, the same face division was made (inner face and outer face), but in this case, the inner face was also separated into two different parts: Inner Face 1 and Inner Face 2 (see Figure 10). Inner Face 1 faces a coil with magnetic flux flowing in the same direction and Inner Face 2 faces an AC coil with flux going in the opposite direction. This distinction has a significant influence on the resulting forces, as can be seen in Figure 10 and Figure 11.

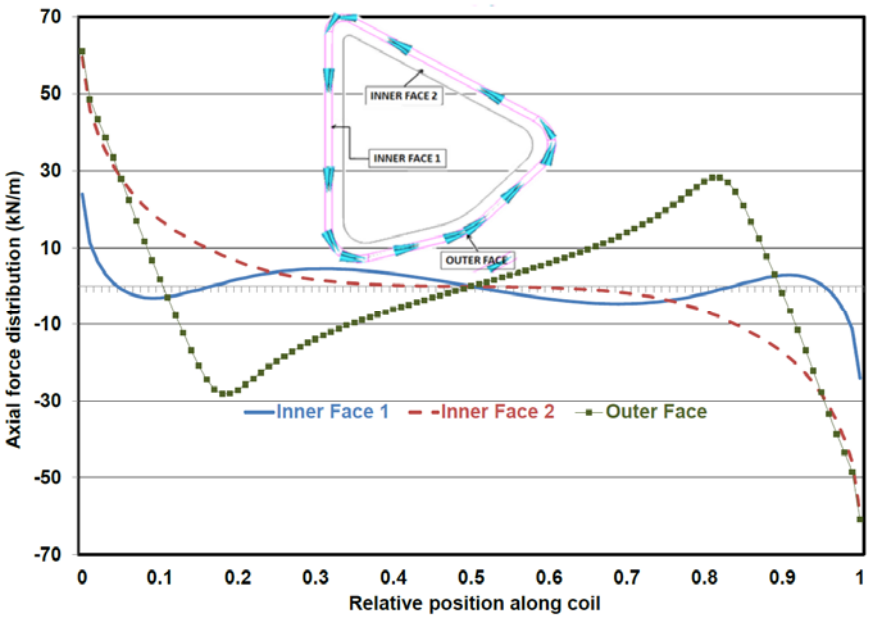

Figure 10 Axial force distribution along the AC coil of the HTS FCL

In order to gain a better understanding of the axial forces, a plot of the cumulative axial force is required. This is shown in Figure 11, which is the integral of the results of the axial force distribution across the length of the AC coils. Negative cumulative axial force implies compression and positive cumulative axial force implies expansion.

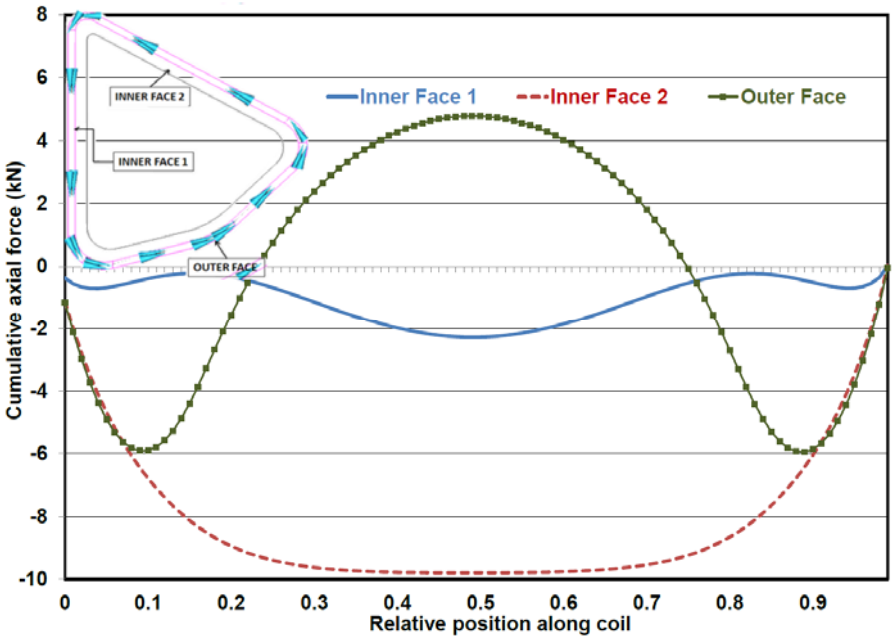

Figure 11 Cumulative axial force along the AC coil of the HTS FCL

IV. COMPARISON AND DISCUSION

The results achieved in this paper show significant differences between the radial forces exerted in the windings of an HTS FCL compared to those of a power transformer. When the current in AC and DC coils are flowing in the same direction (AC current positive), the magnetic field and associated radial forces in the AC coils are increased. The effect is more pronounced in positions close to the DC coils. The DC coils boost the magnetic field, resulting in the two peaks in expansion force shown in Figure 7(a) and a peak in the radial force of 130 kN/m^2 shown in Figure 8. On the other hand, when the current in AC and DC coils is flowing in opposite directions (AC negative current), the radial forces decrease and even change direction at the top and bottom of the coil. Hence, the DC coils are driving the magnetic field to the opposite direction at the top and the bottom of the coil. The currents in the AC coils are attempting to expand them, while the DC coils cause them to compress, resulting in a buckling effect at the ends of the coil. Under a short-circuit condition, each AC coil will therefore suffer a compression-expansion effect. However, the maximum stress will be due to expansion. When

the DC coils are disabled (see Figure 7(b)) the force is lower in the coils and its pattern in the FCL is similar as the one in the power transformer.

Axial forces present the most significant differences between power transformers and HTS FCLs. In the power transformer, the axial forces are compressing the winding longitudinally. The axial force only undergoes a single change in direction at the centre along the coil, as shown in Figure 4. The negative axial force in the top half of the coil implies that the force is exerted downwards, while the positive force in the bottom half exerts an upward force. In the FCL, the axial force for Inner Face 2 shows results similar to those of a power transformer. However, the axial forces on the Outer Face and Inner Face 1 respectively undergo three and five direction changes along the length of the coil, as shown in Figure 10. Figure 11 shows that the Outer Face expands in the centre (positive value of the force) and is subject to compression at the ends of the coil (negative value of force). The net effect will be expansion. The cumulative axial force within Inner Face 1 is changing from expansion to compression along the coil. These phenomena are caused by the magnetic flux originating from the neighbouring coil, where leakage magnetic flux is affecting the resultant force. The resultant force is therefore unbalanced in many turns of the AC coil, because in the same turn the force at the outer face is pushing upwards while the force at the inner face is pushing downwards. This phenomenon is critical for the design of the FCL. Due to its special arrangement, the electromagnetic forces within a high-voltage FCL have to be analysed in detail in order to manufacture a robust device capable of withstanding short-circuit faults.

VI. CONCLUSION

In this paper, electromagnetic forces in power-transformers and HTS FCLs were compared. There are significant differences between the force distribution in a power-transformer and an HTS FCL. These differences will need to be taken into consideration when designing FCLs.

The two peaks in the radial forces shown in Figure 8 necessitate reinforcement of the winding in the affected areas, because an even distribution of support based on the average radial force would no longer be valid. Axial forces also affect design of FCL coils and supports. In power transformers, the spacers which support and distribute the axial forces between the turns of the coil are evenly distributed. In a high-voltage FCL, special consideration is required for the distribution of the spacers to compensate for the imbalance in the axial forces. In the studied example, reinforcement with fibre-belts around AC coils in positions where the radial force peak occurs would be required in order to avoid buckling and hooping. Special distribution of the spacers would also be needed to balance the axial force.

In conclusion, high voltage FCLs require special considerations which need to be analysed thoroughly and independently. Each different configuration in the FCL arrangement will results in unique force distributions, which need to be taken into consideration during the design stage to manufacture a robust device capable of withstanding short-circuit faults.

V. REFERENCES

[1] Moscrop J, Darmann F. Design and development of a 3-Phase saturated core High Temperature Superconducting Fault Current Limiter. International Conference on Electric Power and Energy Conversion Systems, 2009 EPECS '09 2009. p. 1-6.

[2] Moriconi F, De La Rosa F, Singh A, Chen B, Levitskaya M, Nelson A. An innovative compact saturable-core HTS Fault Current Limiter - development, testing and application to transmission class networks. General Meeting of Power and Energy Society, 2010 IEEE2010. p. 1-8.

[3] Branco PJC, Almeida ME, Dente JA. Proposal for an RMS thermoelectric model for a resistive-type superconducting fault current limiter (SFCL). Electric Power Systems Research. 2010;80:1229-39.

[4] Cuixia Z, Shuhong W, Jie Q, Jian GZ, Youguang G, Weizhi G, et al. Transient simulation and analysis for saturated core high temperature superconducting fault current limiter. 12th Biennial IEEE Conference on Electromagnetic Field Computation, CEFC 2006, April 30, 2006 - May 3, 2006. Miami, FL, United states: Institute of Electrical and Electronics Engineers Computer Society; 2006.

[5] Jung BI, Cho YS, Choi HS, Chul DC. The operation stability of a three-phase matrix-type SFCL against break-down of superconducting elements. Physica C: Superconductivity. 2010;470:1636-40.

[6] Morandi A. State of the Art of Superconducting Fault Current Limiters and their Application to the Electric Power System. Physica C: Superconductivity.

[7] Moriconi F, De La Rosa F, Darmann F, Nelson A, Masur L. Development and Deployment of Saturated-Core Fault Current Limiters in Distribution and Transmission Substations. Applied Superconductivity, IEEE Transactions on. 2011;21:1288-93.

[8] A. Nelson FM. 11kV Saturating-Core Inductive FCL for the UK Low-Carbon Network Fund. EPRI Superconductivity Conference. Tallahassee, Florida2011.

[9] Waters M. The Short-Circuit Strength of Power Transformers. London: Macdonald & Co. ; 1966.

[10] Bertagnolli G. Short-circuit duty of power transformers. 3rd ed. Milano: Book printed on behalf of ABB transformatori Legano; 2006.

[11] Kulkarni SV, Khaparde SA. Transformer Engineeering (design and Practice). New York2004.

[12] A. C. de Azevedo ACD, J. C. de Oliveira, B. C. Carvalho, H. de S. Bronzeado. Transformer mechanical stress caused by external short-circuit: a time domain approach. IPST. Jun. 4-7, 2007.

[13] 12.19 WG. The Short Circuit performance of power transformers. CIGRE.Brochure209.

[14] Hiraishi K, Hori Y, Shida S. Mechanical Strength of Transformer Windings Under Short-Circuit Conditions. Power Apparatus and Systems, IEEE Transactions on. 1971;PAS-90:2381-90.

[15] Kulkarni SV, Kumbhar GB. Analysis of Short Circuit Performance of Split-Winding Transformer Using Coupled Field-Circuit Approach. Power Engineering Society General Meeting, 2007 IEEE2007. p. 1-.

[16] McNutt WJ, Johnson WM, Nelson RA, Ayers RE. Power Transformen Short-Circuit Strength - Requirements, Design, and Demonstration. Power Apparatus and Systems, IEEE Transactions on. 1970;PAS-89:1955-69.

[17] McNutt WJ, McMillen CJ, Nelson PQ, Dind JE. Transformer short-circuit strength and standards. IEEE Transactions on Power Apparatus and Systems, . 1975;94:432-43.

[18] Norris ET. Mechanical strength of power transformers in service. Proceedings of the IEE - Part A: Power Engineering. 1957;104:289-300.

[19] Patel MR. Dynamic stability of helical and barrel coils in transformers against axial short - circuit forces. Generation, Transmission and Distribution, IEE Proceedings C. 1980;127:281-4.

[20] Faiz J, Ebrahimi BM, Noori T. Three- and Two-Dimensional Finite-Element Computation of Inrush Current and Short-Circuit Electromagnetic Forces on Windings of a Three-Phase Core-Type Power Transformer. IEEE Transactions on Magnetics. 2008;44:590-7.

[21] K.M. Prasad, K. Davey. Boundary element analysis of team problem no. 20: static force calculation. 4-th International TEAM Workshop, 19931993.

[22] Y. Bulent Yildir BWK, K. M. Prasad. Three dimensional analysis of magnetic fields using the boundary element method. International Coil Winding Conference. Boston1991.
[23] Hall WB, Lopez-Roldan J. Application of rotating arc SF6 interrupter design to the highest distribution voltage levels. Trends in Distribution Switchgear: 400V-145kV for Utilities and Private Networks, 1998 Fifth International Conference on (Conf Publ No 459)1998. p. 145-8.